Visible and near-infrared spectroscopy for distinguishing malignant tumor tissue from benign tumor and normal breast tissues *in vitro*

Yang Zhang
Yongjun Chen
Yuan Yu
Xingbo Xue
Valery V. Tuchin
Dan Zhu

Visible and near-infrared spectroscopy for distinguishing malignant tumor tissue from benign tumor and normal breast tissues *in vitro*

Yang Zhang,[a,b] Yongjun Chen,[c] Yuan Yu,[c,d] Xingbo Xue,[c] Valery V. Tuchin,[e,f,g] and Dan Zhu[a,b]
[a]Huazhong University of Science and Technology, Britton Chance Center for Biomedical Photonics, Wuhan National Laboratory for Optoelectronics, Wuhan 430074, China
[b]Huazhong University of Science and Technology, Department of Biomedical Engineering, Key Laboratory of Biomedical Photonics of Ministry of Education, Wuhan 430074, China
[c]Huazhong University of Science and Technology, Affiliated Tongji Hospital, Wuhan 430030, China
[d]Fudan University, The Fifth People's Hospital of Shanghai, Heqing Road 801, Shanghai 200240, China
[e]Saratov State University, Institute of Optics and Biophotonics, Saratov 410012, Russia
[f]Institute of Precise Mechanics and Control of RAS, Saratov 410028, Russia
[g]University of Oulu, P.O. Box 4500, Oulu 90014, Finland

Abstract. The high incidence and mortality of breast cancer requires an effective, rapid, and cost-effective method for its diagnosis. Here, visible and near-infrared spectroscopy in the wavelength range of 400 to 2200 nm is utilized for distinguishing the malignant tumor tissue from benign tumor and normal breast tissues. Based on the absorption and scattering spectra of fixed samples, three spectral analysis methods are proposed which include an absorption spectral analysis, a scattering spectral analysis, and a combined spectral analysis of the two. By comparison with the histopathological examination, the sensitivity, specificity, and accuracy of the three analysis methods are calculated. The results showed that the combined spectral analysis method can significantly enhance the effectiveness when compared with the sole absorption or scattering spectral analysis method. The sensitivity, specificity, and accuracy of the combined spectral analysis method are 100%, 87.82%, and 87.50% for the benign tumor tissue and 81.82%, 100%, and 87.5% for malignant tumor tissue, respectively. All of the three values are 100% for normal breast tissue. This study demonstrates that the combined spectral analysis method has better potential for *in vitro* optical diagnosis for breast lesions. © *The Authors. Published by SPIE under a Creative Commons Attribution 3.0 Unported License. Distribution or reproduction of this work in whole or in part requires full attribution of the original publication, including its DOI.* [DOI: 10.1117/1.JBO.18.7.077003]

Keywords: breast tissue; breast lesions; visible and near-infrared spectroscopy; combined spectral analysis method; tissue optics; inverse adding-doubling method.

Paper 130044PRR received Jan. 27, 2013; revised manuscript received May 14, 2013; accepted for publication May 21, 2013; published online Jul. 9, 2013.

1 Introduction

Breast cancer is one of the most common malignant tumors for women. The incidence rate of breast cancer has been growing rapidly during the past 10 years. There are almost 1.3 million women suffering from breast cancer each year, and the mortality of breast cancer is up to 40%.[1,2] To reduce the morality, an accurate and efficiency method for early screening of breast cancer is required. Mammography, a common diagnostic technique, has been a common screening tool for breast cancer. However, it is not sensitive to cancerous lesions for radiological dense breasts, which may lead to a significant false-positive reports.[3] Diffuse optical technique based on frequency domain,[4–8] time resolved,[9,10] continuous wave,[11] or the combination[12,13] was used to measure the concentration of oxy-(HbO$_2$) and deoxy-(HbR)hemoglobin to assess the metabolism state of normal or lesion breast, which has shown some potential for noninvasive breast cancer screening.

For some patients, surgery is often unavoidable, but as many as 20% to 70% undergoing breast conserving surgery require repeat surgeries due to a positive-surgical margin diagnosed postoperatively.[14] Until now, the histopathological examination is regarded as the gold standard for the diagnosis of breast lesions based on surgical operation, which can distinguish the malignant tumor from benign tumor and normal breast tissue according to the changes in microscopic morphology and composition of breast tissues by staining methods.[15] However, this method is time consuming. Usually, patients have to wait for three to seven days to get the exact nature of tumor before the surgeons perform mastectomy or lumpectomy.[16,17] With a majority of research efforts focusing on ultraviolet-induced fluorescence,[18] Raman spectroscopy,[19] or optical spectra imaging,[20] optical coherence tomography,[21] the optical biopsy has been used for distinguishing dysplasia and cancer from normal tissue or benign condition as an intraoperative evaluation method.[18–21]

Actually, tissue optical properties, i.e., absorption, scattering, and reduced scattering coefficients, can vary with the degree of tissue lesion severity,[22] which have the potential to aid in the assessment of breast pathology *in vitro*.[23,24] For instance, absorption coefficient reflects molecular composition of tissues, whose changes at specific wavelengths could serve as a spectral fingerprint of the molecular change for the diagnostic purposes.[25] The scattering coefficient or reduced scattering coefficient depends on the size, morphology, and structure of components in tissues. The components of breast tissue include

Address all correspondence to: Dan Zhu, Huazhong University of Science and Technology, Britton Chance Center for Biomedical Photonics, Wuhan National Laboratory for Optoelectronics, Wuhan 430074, China. Tel: 86-27-87792033; Fax: 86-27-87792034; E-mail: dawnzh@mail.hust.edu.cn

blood,[5,12] water,[6,7] lipids,[5,6,8,10] and collagen,[9,10] etc. Variations in the components of lesion tissue would affect absorption and scattering properties, thus providing a means for characterizing the pathological change of tissue.[11] Previous investigations about tissue optics mainly focused on the visible and near-infrared (VIS-NIR) region between 400 and 1000 nm[5–8] and some extended to 1600 nm.[22] It should be noted that the characteristic information of lipids and water in the wavelength range of 1400 to 2000 nm is more significant,[26] which may be more suitable for breast cancer diagnosis.

The purpose of this work is to develop a rapid and effective diagnosis of breast lesions by using VIS-NIR spectral analysis of fixed tissue samples. A commercially available spectrophotometer with an integrating sphere was applied to measure the reflectance and transmittance of the samples. Based on the absorption and scattering spectra of normal and abnormal breast tissues in the wavelength range of 400 to 2200 nm, an absorption spectral or scattering analysis methods were proposed by self-defined absorption spectrum variation factor A or a wavelength exponent c of scattering. Further, a combined spectral analysis of the two parameters was developed. By comparing the results of spectral analysis methods with histopathological examination, the sensitivity, specificity, and accuracy were calculated to evaluate the effectiveness of the methods.

2 Materials and Methods

2.1 Experimental System

In order to obtain the optical properties of tissue, a spectrophotometer (Lambda 950, PerkinElmer, Waltham, Massachusetts) with an integrating sphere was applied to measure the transmittance and reflectance spectrums of the samples in the range of 400 to 2200 nm with 10-nm intervals. Here, the diameter of the integrating sphere is 150 mm, and the diameter of the sample port is 25.4 mm. This commercial spectrophotometer has high accuracy and repeatability, which were proved previously.[27–29] Therefore, in this work, a single measurement of transmittance or reflectance spectrum for each sample was performed, respectively. The transmittance and reflectance were measured in the range of 400 to 2200 nm with a 10-nm interval.

2.2 Sample Preparation

All samples were obtained from 28 patients during surgery in Affiliated Tongji Hospital, Huazhong University of Science and Technology. According to the histopathological report, the samples were divided into three groups: malignant breast tumor tissue ($n = 11$), benign breast tumor tissue ($n = 5$), and normal breast tissue ($n = 16$). Normal breast tissue samples were obtained from safe margins of tumors without obvious tumor characteristics, which were confirmed by histopathology. After having removed the residual blood on the tissue surface with saline, the fresh breast tissues were fixed immediately in 10% formaldehyde solution so as to keep their nanoarchitecture.[30,31] Fixed tissues were stored in a dark room at 4°C, then warmed up to 25°C, and sliced into tissue sections before measurements. The size of each sample was approximately 30×30 mm² to assure it was larger than the sample port (25.4×25.4 mm²) of the integrating sphere. Each sample was sandwiched between two glass slides with 1 mm thickness each, and measured four

times with a caliper on different points and averaged. The average thickness of samples was 1.1 ± 0.34 mm.

2.3 Data Analysis

Based on the measurements of sample thickness, transmittance and reflectance spectra in the range of 400 to 2200 nm and the corresponding spectra of absorption coefficient and reduced scattering coefficient were calculated by the inverse adding-doubling (IAD) method. This arithmetic was developed by Prahl et al.,[32,33] which has been widely applied to derive tissue optical properties.[26–29,34,35] In order to find some effective optical markers to characterize different types of breast tissues, further analysis was performed as in the following sections.

2.3.1 Absorption and scattering spectral analysis methods

Since there are typical absorption peaks at 1450 nm for water and 1720 nm for lipid,[26] a new parameter, namely the absorption spectrum variation factor A, was defined as follows:

$$A = \frac{\mu_{a1450\ nm} - \mu_{a1720\ nm}}{\mu_{a1450\ nm} + \mu_{a1720\ nm}}. \tag{1}$$

Here, $\mu_{a1450\ nm}$ and $\mu_{a1720\ nm}$ are the absorption coefficients of breast tissue at 1450 and 1720 nm, respectively.

In general, the reduced scattering coefficient of tissue includes the total contribution of Rayleigh and Mie scatterings, which can be described with the following equation:[26]

$$\mu_s'(\lambda) = a_{Rayl}\left(\frac{\lambda}{1\ nm}\right)^{-4} + b_{Mie}\left(\frac{\lambda}{1\ nm}\right)^c. \tag{2}$$

Here, a_{Rayl} and b_{Mie} indicate the part of the Rayleigh and the Mie scatterings, respectively, λ is the wavelength, and c is the wavelength exponent. Equation (2) was used to curve fit the reduced scattering spectra of tissue in the wavelength range of 400 to 2200 nm, and then the optimal parameters would be calculated by using the least square regression.

In order to further improve the effectiveness of spectral analysis methods for distinguishing malignant tumor tissue from benign tumor and normal human breast tissues, a combined analysis method of the above two parameters was performed as follow: first, the absorption spectrum variation factor A was used to distinguish the normal samples from the diseased breast tissues. Second, the wavelength exponent c was applied to classify the diseased ones into two categories, benign and malignant tumors.

2.3.2 Statistical analysis

A one-factor analysis of variance (ANOVA) was applied to determine the significant difference of the absorption spectrum variation factor A or the wavelength exponent c of different types of breast tissues by SPSS16.0 software. Changes were considered to be significant if $P < 0.05$ and extremely significant if $P < 0.01$.

2.3.3 Effectiveness analysis

The effectiveness of the VIS-NIR spectral analysis methods is determined by comparing the results with histological examination. Based upon the results of these comparisons, three quantitative values (sensitivity, specificity, and accuracy) can

be calculated to provide an objective comparison of various spectral analysis methods. Calculation of the three quantities depends upon classifying a particular analysis as either a true positive (TP), which represents classification by both techniques as lesion; a false positive (FP), which corresponds to a classification as lesion by spectroscopy and as normal by histology; a false negative (FN), which corresponds to a normal classification by spectroscopy and a lesion classification by histology; or a true negative (TN), which corresponds to classification by both techniques as normal. Once the appropriate classifications have been performed, sensitivity, specificity, and accuracy for discrimination of benign and malignant tumors are calculated as follows:[15]

$$\begin{cases} \text{Sensitivity} = \text{TP}/(\text{TP} + \text{FN}) \\ \text{Specificity} = \text{TN}/(\text{TN} + \text{FP}) \\ \text{Accuracy} = (\text{TP} + \text{TN})/(\text{TP} + \text{TN} + \text{FP} + \text{FN}) \end{cases}. \quad (3)$$

3 Results

3.1 Absorption Spectra of Normal and Diseased Human Breast Tissues

Figure 1(a)–1(c) shows the absorption spectra of normal breast tissue samples ($n = 16$), benign tumor tissue samples ($n = 5$), and malignant tumor tissue samples ($n = 11$) in the range of 400 to 2200 nm. It can be seen that the absorption spectra have good consistency in the same type of breast tissue, but differences exist in different types of tissues.

Figure 1(a) shows that there are four absorption peaks at 1190, 1450, 1720, and 1930 nm for normal breast tissue. The strongest absorption peak occurs at 1930 nm, and the weakest absorption peak at 1190 nm. Comparing with Fig. 1(b) and 1(c), both the absorption peaks of benign and malignant breast tumor tissues at 1450 and 1930 nm are larger than those of normal tissue, but the peak of diseased breast tissues at 1720 nm almost disappears.

Table 1 summarizes the mean absorption coefficients at 1190, 1450, 1720, and 1930 nm for different types of breast tissues and the mean absorption spectrum variation factor A according to the Eq. (1). The statistical analysis shows that there are significant differences in the absorption peaks at 1450, 1930, and 1720 nm between normal and diseased breast tissues except at 1190 nm, but no significant differences in the peaks at the above four wavelengths between malignant and

benign breast tissues. In contrast, the absorption spectrum variation factor A defined in this work indicates an extremely significant difference between normal and diseased breast tissues and a significant difference between benign and malignant breast tissues.

### 3.2 Scattering Spectra of Normal and Diseased Human Breast Tissues

Figure 2(a)–2(c) shows that the scattering spectra of all the samples are very similar for the same type of breast tissue but different for different types of tissues. In visible wavelengths, the reduced scattering coefficient of normal breast tissue samples is much smaller than that of diseased tissues, and the values of malignant tumor tissue is the biggest. In addition, there are two scattering peaks at 1450 and 1940 nm for diseased tissues.

The mean $\pm$ standard error of wavelength exponent c for different types of breast tissues was calculated, and further one-factor ANOVA was performed to test the differences among the three types of breast tissues. The results are summarized in Table 2. It can be found that significant differences not only exist between the normal breast and diseased breast tissues, but also exist between benign and malignant tumor tissues.

3.3 Effectiveness of Spectral Analysis Methods

Figure 3 shows the distribution of absorption spectrum variation factor A and wavelength exponent value c of scattering for all of the samples. It can be found that it is easy to distinguish the normal and diseased breast because the normal samples are mainly localized in areas I and II, but difficult to distinguish the benign and malignant breast tissues because there is overlap in areas III and IV.

The combined analysis method ($A \& c$) of the absorption and scattering spectral analysis was performed to distinguish malignant tumor, benign tumor, and normal human breast samples from each other. First, when the value of A was less than 0.058 (median of limit error of A for normal and benign tumor, 99% confidence interval), the sample was defined as normal, otherwise, the sample was defined as diseased tissue. Second, the wavelength exponent c is applied to classify the types of diseased samples as benign or malignant tumor. According to the distribution of wavelength exponent c of scattering, the sample was defined as a benign tumor one when the value of c was greater than −0.829 (median of limit error of c for benign and malignant tumor, 99% confidence interval), otherwise, the sample was defined as a malignant tumor.
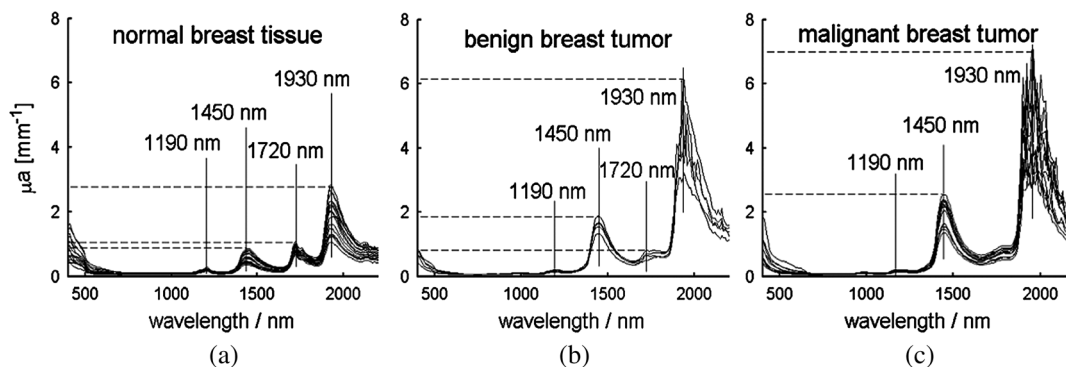
Fig. 1 Absorption spectra of different samples in the range of 400 to 2200 nm. (a) Normal breast tissue, (b) benign breast tumor tissue, and (c) malignant breast tumor tissue.
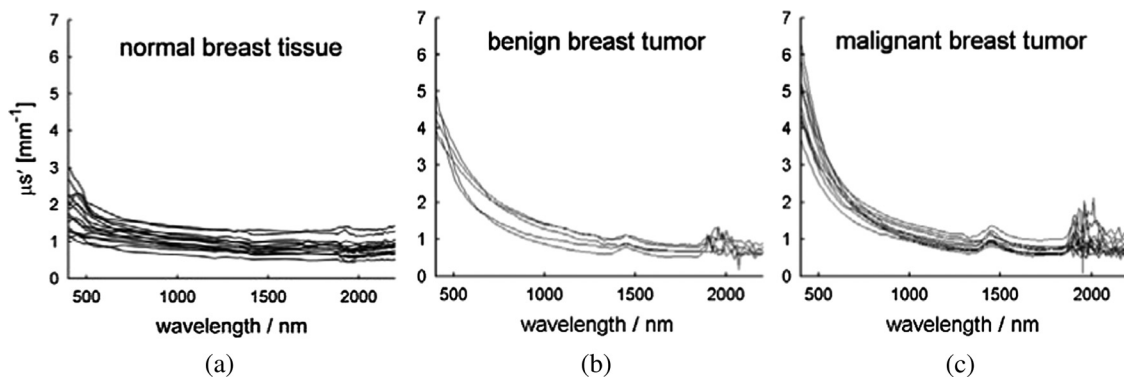
Table 1 Absorption parameters of different types of breast tissues.

Breast tissue	Normal ($n = 16$)	Benign ($n = 5$)	Malignant ($n = 11$)
μ_a ($\lambda = 1190$ nm)	0.0836 ± 0.0042	0.0803 ± 0.0062	0.0836 ± 0.0032
μ_a ($\lambda = 1450$ nm)	0.6686 ± 0.0418	1.3402 ± 0.0912	1.8864 ± 0.1272
μ_a ($\lambda = 1720$ nm)	0.8766 ± 0.0308	0.6598 ± 0.0504	0.6208 ± 0.0336
μ_a ($\lambda = 1930$ nm)	1.9093 ± 0.1363	4.4220 ± 0.5195	4.2260 ± 0.2940
A_i	-0.1346 ± 0.0194	0.3402 ± 0.0538	0.5048 ± 0.0218
$A_i - A_{i,normal}$	—	0.4748^a	0.6394^a
$A_i - A_{i,benigntumor}$	—	—	0.1646^b

Note: A_i is the mean $\pm$ standard error of A.
[a]Extremely significant difference ($P < 0.01$).
[b]Significant difference ($P < 0.05$).

Fig. 2 The reduced scattering coefficient spectrum of different samples in the range of 400 to 2200 nm. (a) Normal breast tissue, (b) benign breast tumor tissue, and (c) malignant breast tumor tissue.

Table 2 The wavelength exponent values of scattering of different types of breast tissues.

| Breast tissue	Normal ($n = 16$)	Benign ($n = 5$)	Malignant ($n = 11$)
c_i	-0.4730 ± 0.0530	-0.7170 ± 0.0456	-0.9798 ± 0.0598
$c_i - c_{i,normal}$		-2440^a	-0.5056^b
$c_i - c_{i,benigntumor}$			-0.2628^a

Note: c_i is the mean $\pm$ standard error of c.
[a]$p < 0.05$.
[b]$p < 0.01$.

In order to evaluate the effectiveness of the absorption, scattering, or the integrating spectral analysis methods, the type identification of spectroscopy for each sample was assessed whether it is a TP, FN, TN, or FP by comparing the calculated value of optical parameters (A, c, or A & c) and the result of histopathological examination. The sensitivity, specificity, and accuracy were calculated by using Eq. (3).[15] The results are summarized in Table 3. Among the three spectral analysis methods, the combined spectral analysis method has the highest sensitivity and accuracy for discrimination of benign breast tumor tissue which reach up to 100% and 87.50%, respectively. The specificity is slightly lower than that for absorption spectral analysis, but higher than that for scattering spectral analysis. For discrimination of malignant breast tumor tissue, the specificity of integrating analysis method is 100%, which is higher than those for the two other methods; the sensitivity is 81.82%, which is the same as that of the higher of the sole analysis methods; and the accuracy has the same as that for absorption spectral analysis, which is slightly lower than that from scattering spectral analysis method.
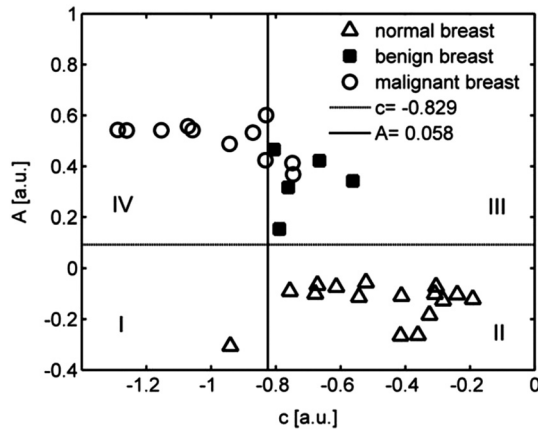
Fig. 3 Distribution of absorption spectrum variation factor A and wavelength exponent value c of scattering of different types of breast tissues.

4 Discussion

From the above measurements, it was found that there are differences in absorption and scattering spectra among the normal, benign, and malignant breast tissues. For instance, there is a characteristic peak at 1720 nm for normal breast tissue, while the peak almost disappears for diseased tissues. This should be due to the changes in stroma of breast tissue.[24] It is well known that a large amount of fat cells exist in normal breast tissue, but only a few in benign breast tumor tissue, and even fewer in malignant breast tumor tissue. Instead, there is a lot of collagenous stroma in lesion breast tissue.[24,36] As the main component of fat, the lipid has a characteristic absorption peak at 1720 nm,[26] so the changes in absorption peak at 1720 nm reflect the content change of fat cells in breast tissue.

In the view of histopathology, the water content of a fat cell is much lower than that of fibrocyte of tumor stroma.[37] Therefore, water is regarded as an important indicator of breast lesion. Chung et al. found the increase of water content in diseased breast tissues with diffuse optical spectroscopy.[7] It is reported

Table 3 Effectiveness of spectral analysis for distinguishing different types of breast tissues.

Type of tissues	Spectral analysis	Sensitivity (%)	Specificity (%)	Accuracy (%)
Normal	A	100.00	100.00	100.00
	C	68.75	93.75	84.38
	$A \& c$	100.00	100.00	100.00
Benign	A	80.00	88.89	81.25
	C	80.00	74.07	75.00
	$A \& c$	100.00	81.82	87.50
Malignant	A	72.73	95.24	87.50
	C	81.82	95.24	90.63
	$A \& c$	81.82	100.00	87.50

Note: A means the absorption spectral analysis method, c means the scattering spectral analysis method, and $A \& c$ means the combined spectral analysis method.

that in the wavelength range of 1100 to 2000 nm, water has three main absorption peaks at 1190, 1450, and 1930 nm, respectively.[26] Compared to the two absorption coefficient magnitudes at 1450 and 1930 nm, the value at 1190 nm is too small to show an obvious peak. This explains why there is no significant difference at 1190 nm between normal and diseased breast tissues. The latter two peaks at 1450 and 1930 nm show significant differences between normal and diseased breast tissues, but it was still unable to separate the benign and malignant tumor. Although the absorption peak of breast tissue at 1930 nm is higher than the one at 1450 nm, there is bigger noise for absorption coefficient measurement when the wavelength is longer than 1880 nm. It may be caused by different types of water in tissues. As we know, water usually has two states: free water and bound water. Free water has three absorption peaks at 1892, 1906, and 1924 nm, while the bound water has two absorption peaks at 1909 and 1927 nm.[38] In addition, the reflectance of the integrating sphere wall decreases with increasing wavelength, which increases the variation of measurements. Therefore, considering the absorption characteristics of water at 1450 nm and lipid at 1720 nm, the defined absorption spectrum variation factor A makes it possible to characterize different types of breast tissues. For future work, this complex band with a center at 1930 nm should be analyzed more precisely because it contains potential information about free and bound water,[38] which could be additional intrinsic markers of tissue malignancy.[7] Moreover, the content of each component, even for healthy breast tissue, is not identical for different persons or different ages,[11] so the single absorption spectral analysis is insufficient to accurately characterize the type of breast tissues.

The previous investigations showed that the content of collagen has potential implications for the assessment of breast density and cancer risk,[7] which may be used to describe the changes of nanoarchitecture in stroma among the three types of breast tissues according to the scattering spectra. The results show that there is an obvious difference in scattering spectra among normal and lesion breast tissues in the spectrum of visible light, i.e., the reduced scattering coefficient of normal breast is much smaller than the diseased ones, and the value of malignant tumor is the largest, but there is no evident difference in the range of 1000 to 2200 nm. It can be interpreted as follows: the collagenous stroma in benign tumor and the hyperplasia of fibrous connective tissue in malignant tumor will increase Mie scattering of tissue. Lipid, an important source of Mie scattering, disappears with the lesion of breast tissue, which decreases the scattering. The increase of collagenous stroma and the decrease of lipid produce opposite contributions to the scattering of lesion breast tissues for the longer wavelength. However, both fibrous connective and collagenous stromal tissue consist of microfibrils with a period of 64 nm, which results in strong Rayleigh scattering.[39,40] Therefore, for the visible light, the reduced scattering coefficient of lesion breast is much higher than that of normal breast. Because there are numerous of hyperplasia of dense fibrous connective tissue in malignant tumor, it leads to a stronger Rayleigh scattering than that in benign tumor. In this study, the introduced wavelength exponent c based on the size of scatters can be used to describe the scattering characteristic of different types of breast tissues. There are two scattering peaks at 1450 and 1930 nm for the benign or malignant breast tissues, which should be due to a cross-talk between the calculated reduced scattering coefficient and the absorption coefficient. Since it has been proved that the strong absorption

raises the calculated value of reduced scattering coefficient by the IAD algorithm,[26,34,35] the scattering spectral analysis neglects the information.

In order to evaluate the effectiveness of a diagnosis technique, the statistical analysis is commonly applied to test the significant difference between normal or lesion tissues based on lots of samples. For one testing sample, clinicians are more concerned about the sensitivity, specificity, and accuracy of the technique. In this work, not only the statistical analysis of two self-defined parameters was tested, but also the effectiveness of various spectral analysis methods was evaluated. Taking the above results into consideration, the combined analysis method of the absorption and scattering spectra is superior compared to the sole absorption or scattering spectral analysis method.

With the development of various optical techniques, optical biopsy shows potential in the diagnosis of breast tumor,[41,42] which depends strongly on the accuracy of tissue optical properties. *In vivo* measurements are the most powerful evidence to disease diagnosis, yet still suffer from limited information on tissue optical properties. Fixed tissue is different from *in vivo* condition. For instance, the information of blood oxygen saturation is lost with this method, yet some important information is kept such as content of water and lipid. Besides, the morphology of tissue can be kept which is also the first procedure of the histology. The VIS-NIR spectroscopy based on fixed tissues demonstrates some abilities to distinguish malignant tumor tissue from benign tumor and normal human breast tissues, which will provide significant reference for optical biopsy.

Until now, surgeons always wait for the results of histopathological diagnosis before they decide to perform a mastectomy. It usually takes several days, because the time-consuming process includes about 50 steps. For instance, it spends 24 h on tissue fixation and 15 h on dehydration. The tissue block is then sliced by microtome and heated to fix slices on microscope slides, and then stained by hematoxylin-eosin. If the immunohistochemistry staining is used, the patient needs to wait for a longer time. Before microscopic examination, the slice should be sealed.[21] In addition, the microscopic examination depends on the judgment of the pathologist, which suffers from subjective factors and experience. In contrast, the proposed spectral analysis method is based on the integrating sphere technique and IAD algorithm, which could provide objective values of absorption coefficient and reduced scattering coefficient of fixed tissues. As an *in vitro* diagnosis technique, this optical method is more time efficient than the histopathological examination.

It should be noticed that there are some limitations for the current study. For the integrating sphere technique, the size of the excised tissue block should be larger than the sample port of the integrating sphere. In addition, the accuracy of optical properties of the sample is relative to the homogeneity of the sample. Fortunately, it is not difficult to obtain larger breast tissues. In addition, the number of samples is relatively low in this work, which may influence categorization of the range of optical parameters (A, c, and A & c) for distinguishing malignant tumor tissue from benign tumor and normal breast tissues. Future studies would be necessary to further evaluation of the sensitivity, specificity, and accuracy of the developed spectral analysis method by testing large numbers of samples.

5 Conclusions

Based on the measurements of VIS-NIR spectra of fixed samples *in vitro*, a new combined spectral analysis method of

absorption and scattering parameters was proposed to distinguish malignant tumor tissue from benign tumor and normal human breast tissues. Comparing with the histopathological examination, the effectiveness of the method was evaluated by calculating the sensitivity, specificity, and accuracy, respectively. The results show that the sensitivity, specificity, and accuracy can reach up to 100% for normal breast tissue, to 100%, 87.82%, and 87.50% for benign breast tumor, respectively, and to 81.82%, 100%, and 87.5% for malignant breast tumor, respectively. The combined spectral analysis method can significantly enhance the effectiveness as compared with sole absorption or scattering spectrum analysis method. This method is effective, simple, rapid, and cost effective, which may become a helpful alternative method for *in vitro* diagnosis of breast lesions.

References

1. J. Ferlay et al., "Estimates of worldwide burden of cancer in 2008: GLOBOCAN 2008," *Int. J. Cancer* **127**(12), 2893–2917 (2010).
2. R. Siegel, D. Naishadham, and A. Jemal, "Cancer statistics, 2012," *CA Cancer J. Clin.* **62**(1), 10–29 (2012).
3. R. A. Hubbard et al., "Cumulative probability of false-positive recall or biopsy recommendation after 10 years of screening mammography," *Ann. Intern. Med.* **155**(8), 481–492 (2011).
4. S. Fantini et al., "Assessment of the size, position, and optical properties of breast tumors *in vivo* by noninvasive optical methods," *Appl. Opt.* **37**(10), 1982–1989 (1998).
5. B. J. Tromberg et al., "Non-invasive *in vivo* characterization of breast tumor using photon migration spectroscopy," *Neoplasia* **2**(1–2), 26–40 (2000).
6. T. O. McBride et al., "Multispectral near-infrared tomography: a case study in compensating for water and lipid content in hemoglobin imaging of the breast," *J. Biomed. Opt.* **7**(1), 72–79 (2002).
7. S. H. Chung et al., "*In vivo* water state measurements in breast cancer using broadband diffuse optical spectroscopy," *Phys. Med. Biol.* **53**(23), 6713–6727 (2008).
8. S. Kukreti et al., "Characterization of metabolic differences between benign and malignant tumors: high-spectral-resolution diffuse optical spectroscopy," *Radiology* **254**(1), 277–284 (2010).
9. P. Taroni et al., "Absorption of collagen: effects on the estimate of breast composition and related diagnostic implications," *J. Biomed. Opt.* **12**(1), 014021 (2007).
10. P. Taroni et al., "Diffuse optical spectroscopy of breast tissue extended to 1100 nm," *J. Biomed. Opt.* **14**(5), 054030 (2009).
11. N. Shah et al., "Spatial variations in optical and physiological properties of healthy breast tissue," *J. Biomed. Opt.* **9**(3), 534–540 (2004).
12. C. Zhou et al., "Diffuse optical monitoring of blood flow and oxygenation in human breast cancer during early stages of neoadjuvant chemotherapy," *J. Biomed. Opt.* **12**(5), 051903 (2007).

13. J. Wang et al., "*In vivo* quantitative imaging of normal and cancerous breast tissue using broadband diffuse optical tomography," *Med. Phys.* **37**(7), 3715–3724 (2010).

14. L. Jacobs, "Positive margins: the challenge continues for breast surgeons," *Ann. Surg. Oncol.* **15**(5), 1271–1272 (2008).

15. T. Vo-Dinh and B. M. Cullum, "Fluorescence spectroscopy for biomedical diagnostics," Chapter 28 in *Biomedical Photonics Handbook*, T. Vo-Dinh, Ed., pp. 19–25, CRC Press, Boca Raton, FL (2003).

16. L. B. Rorke, "Pathologic diagnosis as the gold standard cancer," *Cancer* **79**(4), 665–667 (1997).

17. G. Sainte-Marie, "A paraffin embedding technique for studies employing immunofluorescence," *J. Histochem. Cytochem.* **10**(3), 250–256 (1962).

18. N. Tagaya et al., "Intraoperative identification of sentinel lymph nodes by near-infrared fluorescence imaging in patients with breast cancer," *Am. J. Surg.* **195**(6), 850–853 (2008).

19. A. S. Haka et al., "*In vivo* margin assessment during partial mastectomy breast surgery using Raman spectroscopy," *Cancer Res.* **66**(6), 3317–3322 (2006).

20. T. M. Bydlon et al., "Performance metrics of an optical spectral imaging system for intra-operative assessment of breast tumor margins," *Opt. Express* **18**(8), 8058–8076 (2010).

21. F. T. Nguyen et al., "Intraoperative evaluation of breast tumor margins with optical coherence tomography," *Cancer Res.* **69**(22), 8790–8796 (2009).

22. R. Nachab´e et al., "Diagnosis of breast cancer using diffuse optical spectroscopy from 500 to 1600 nm: comparison of classification methods," *J. Biomed. Opt.* **16**(8), 087010 (2011).

23. T. T. Le, T. B. Huff, and J. Cheng, "Coherent anti-Stokes Raman scattering imaging of lipids in cancer metastasis," *BMC Cancer* **9**(1), 42 (2009).

24. T. T. Le et al., "Nonlinear optical imaging to evaluate the impact of obesity on mammary gland and tumor stroma," *Mol. Imag.* **6**(3), 205–211 (2007).

25. G. R. Hunt, "Spectral signatures of particulate minerals in the visible and near infrared," *Geophysics* **42**(3), 501–513 (1977).

26. A. N. Bashkatov et al., "Optical properties of human skin, subcutaneous and mucous tissues in the wavelength range from 400 to 2000 nm," *J. Phys. D Appl. Phys.* **38**(15), 2543–2555 (2005).

27. X. Wen et al., "Controlling the scattering of intralipid by using optical clearing agents," *Phys. Med. Biol.* **54**(22), 6917–6930 (2009).

28. T. Yu et al., "Quantitative analysis of dehydration in porcine skin for assessing mechanism of optical clearing," *J. Biomed. Opt.* **16**(9), 095002 (2011).

29. Y. Zhang et al., "The accuracy of a commercial spectrophotometer with single integrating sphere for measuring optical properties of turbid sample," *Proc. SPIE* **7562**, 756219 (2010).

30. K. Ostrowski, J. Komender, and K. Kwarecki, "Quantitative investigations on the solubility of proteins extracted from tissues fixed by different chemical and physical methods," *Cell. Mol. Life Sci.* **17**(4), 183–184 (1961).

31. R. C. Roozemond, "Thin layer chromatographic study of lipid extraction from cryostat sections of rat hypothalamus by some fixatives," *J. Histochem. Cytochem.* **15**(9), 526–529 (1967).

32. J. W. Pickering et al., "Double-integrating-sphere system for measuring the optical properties of tissue," *Appl. Opt.* **32**(4), 399–410 (1993).

33. S. A. Prahl, M. J. C. Van Gemert, and A. J. Welch, "Determining the optical properties of turbid media by using the adding-doubling method," *Appl. Opt.* **32**(4), 559–568 (1993).

34. D. Zhu, Q. Luo, and J. Cen, "Effects of dehydration on the optical properties of *in vitro* porcine liver," *Lasers Surg. Med.* **33**(4), 226–231 (2003).

35. D. Zhu et al., "Effect of light losses of sample between two integrating spheres on optical properties estimation," *J. Biomed. Opt.* **12**(6), 064004 (2007).

36. Z. M. Shao, M. Nguyen, and S. H. Barsky, "Human breast carcinoma desmoplasia is PDGF initiated," *Oncogene* **19**(38), 4337–4345 (2000).

37. L. W. Horn, E. M. Rogus, and K. L. Zierler, "Water content of isolated fat cells," *BBA Gen Subjects* **313**(2), 399–402 (1973).

38. K. A. Martin, "Direct measurement of moisture in skin by NIR spectroscopy," *J. Soc. Cosmet. Chem.* **44**(5), 249–261 (1993).

39. I. S. Saidi, S. L. Jacques, and F. K. Tittel, "Mie and Rayleigh modeling of visible-light scattering in neonatal skin" *Appl. Opt.* **34**(31), 7410–7418 (1995).

40. S. L. Jacques, "Fractal nature of light scattering in tissues," *J. Innovat. Opt. Health Sci.* **4**(1), 1–7 (2011).

41. Y. Yu et al., "Near-infrared, broad-band spectral imaging of the human breast for quantitative oximetry: applications to healthy and cancerous breasts," *J. Innovat. Opt. Health Sci.* **3**(4) 267–277 (2010).

42. T. T. Le and J. Cheng, "Non-linear optical imaging of obesity-related health risks: review," *J. Innovat. Opt. Health Sci.* **2**(1), 9–25 (2009).